



Individual aerosol particles in and below clouds along a Mt. Fuji slope: Modification of sea-salt-containing particles by in-cloud processing

S. Ueda^{a,*}, Y. Hirose^{a,2}, K. Miura^a, H. Okochi^b

^a Faculty of Science, Tokyo University of Science, Tokyo, Japan

^b Faculty of Science and Engineering, Waseda University, Tokyo, Japan

ARTICLE INFO

Article history:

Received 23 April 2013

Received in revised form 10 October 2013

Accepted 12 October 2013

Available online 18 October 2013

Keywords:

Atmospheric aerosol particles

Electron micrograph

In-cloud process

Sea salt particle

Atmospheric aging

Mountain site

ABSTRACT

Sizes and compositions of atmospheric aerosol particles can be altered by in-cloud processing by absorption/adsorption of gaseous and particulate materials and drying of aerosol particles that were formerly activated as cloud condensation nuclei. To elucidate differences of aerosol particles before and after in-cloud processing, aerosols were observed along a slope of Mt. Fuji, Japan (3776 m a.s.l.) during the summer in 2011 and 2012 using a portable laser particle counter (LPC) and an aerosol sampler. Aerosol samples for analyses of elemental compositions were obtained using a cascade impactor at top-of-cloud, in-cloud, and below-cloud altitudes. To investigate composition changes via in-cloud processing, individual particles (0.5–2 μm diameter) of samples from five cases (days) collected at different altitudes under similar backward air mass trajectory conditions were analyzed using a transmission electron microscope (TEM) equipped with an energy dispersive X-ray analyzer. For most cases (four cases), most particles at all altitudes mainly comprised sea salts: mainly Na with some S and/or Cl. Of those, in two cases, sea-salt-containing particles with Cl were found in below-cloud samples, although sea-salt-containing particles in top-of-cloud samples did not contain Cl. This result suggests that Cl in the sea salt was displaced by other cloud components. In the other two cases, sea-salt-containing particles on samples at all altitudes were without Cl. However, molar ratios of S to Na (S/Na) of the sea-salt-containing particles of top-of-cloud samples were higher than those of below-cloud samples, suggesting that sulfuric acid or sulfate was added to sea-salt-containing particles after complete displacement of Cl by absorption of SO_2 or coagulation with sulfate. The additional volume of sulfuric acid in clouds for the two cases was estimated using the observed S/Na values of sea-salt-containing particles. The estimation revealed that size changes by in-cloud processing from below-cloud to top-of-cloud altitudes were less than 6% for sizes of 0.5–2 μm diameter. The obtained results will be useful to evaluate the aging effect and transition of aerosol particles through in-cloud processing.

© 2013 Elsevier B.V. All rights reserved.

1. Introduction

Atmospheric aerosol particles play an important role in determining climate effects by their direct scattering and absorption of solar radiation while acting indirectly as cloud

condensation nuclei (CCN) (e.g., Haywood and Boucher, 2000; Pilinis et al., 1995; Twomey, 1977). For estimation of their optical properties and characteristics of CCN, the size, concentration, and composition of aerosol particles are fundamental parameters, but they can be modified in the atmosphere by atmospheric aging and scavenging processes. Atmospheric aging processes of aerosol particles include adsorption and condensation of semi-volatile vapors, coagulation of particles with other pre-existing aerosol particles, heterogeneous reactions at the particle surface with gaseous species, and in-cloud processing in the atmosphere (Fuchs, 1964; Husar and Whitby, 1973;

* Corresponding author at: Solar-Terrestrial Environment Laboratory, Nagoya University, Furo-cho, Chikusa-ku, Nagoya 464-8601, Japan.

¹ Presently at Solar-Terrestrial Environment Laboratory, Nagoya University, Nagoya, Japan.

² Presently at Graduate School of Environmental Studies, Nagoya University, Nagoya, Japan.

Mamane and Gottlieb, 1989; Meng and Seinfeld, 1994). In-cloud processing is absorption/adsorption of gaseous and particulate materials of activated particles as CCN.

The mass–size distribution of aerosols and their components (e.g., sulfate, elemental carbon and organic matter) is often observed as a bimodal distribution with mode peaks in less than 0.5 μm (condensation mode) and greater than 0.5 μm (droplet mode) (e.g., Huang and Yu, 2008; Meng and Seinfeld, 1994; Xiao et al., 2009). Generally, condensation, coagulation and heterogeneous reactions can modify the particle size to 300 nm at best. Consequently, droplet mode particle formation is regarded as a result of in-cloud processing. Meng and Seinfeld (1994), Kerminen and Wexler (1995), and Huang and Yu (2008) demonstrated numerically that in-cloud formation of sulfate is the only possible mechanism for growth of condensation mode particles to droplet mode particles. Although these studies were based on numerical analyses and ground-level observations of aerosol size distribution, some observations at sites near clouds have been conducted to investigate aerosol changes via in-cloud processing. The modification of the aerosol size distribution by in-cloud processing was traced empirically upwind, inside, and downwind from a hill-cap cloud in ground-based cloud passage experiments at Great Dun Fell, United Kingdom (Birmili et al., 1999; Bower et al., 1997; Choulaton et al., 1997), on Tenerife, Spain (Bower et al., 2000), and at Mt. Thüringer Wald, Germany (Mertes et al., 2005). By comparing the upwind and downwind dry particle size distributions, differences in aerosol sizes were undetectable for particles with diameters greater than 300 nm. One reason might be that their relative diameter increase by the addition of soluble mass is smaller, and that the size distribution was affected by deposition along the forest canopy as dominating loss processes. Such reports underscore the difficulty of assessing the changes of size distribution of droplet particles in actual clouds.

In-cloud processing has been regarded as an effective process among aging processes of aerosol particles, but discussions of quantitative changes in actual clouds remain poor. However, several studies have assessed the compositional change of aerosol particles using individual particle analysis with electron microscopy (e.g., Nimura et al., 1998; Pósfai et al., 2003; Ueda et al., 2011a). Nimura et al. (1998) reported that some Asian dust particles obtained at Nagasaki were internally mixed with sea salt. They compared cloud conditions along the transport path based on satellite and trajectory, and reported that such dust particles containing sea salt were present abundantly in a case in which the air would have been influenced strongly by clouds in the maritime atmosphere during transport. Recent studies using microscopic analysis and based on field observations by aircraft or at high alpine sites have shown the composition of individual particles in clouds (Kojima et al., 2004; Kojima and Buseck, 2005; Li et al., 2011; Matsuki et al., 2010; Twohy and Anderson, 2008; Ueda et al., 2011b). Particularly, Matsuki et al. (2010) described differences of mixing states of sulfate, chloride, and nitrate on dust particles in and out of clouds, and suggested that the secondary species were particularly enhanced by in-cloud processing. As previous reports have described, some composition of individual particles can yield information about changes in particles caused by in-cloud processing. Using compositions of individual particles as the tracer, differences for particles before and after undergoing in-cloud processes might be assessed more quantitatively. However, details of

comparisons of particles obtained before and after in-cloud processing have not been described in reports of those previous studies.

In this study, to elucidate the effects of processing in actual clouds, we conducted atmospheric observations along the slope of Mt. Fuji, Japan. Aerosol samples for microscopic analysis using electron dispersive X-ray were obtained in and below clouds, as particles before and after in-cloud processing. This paper presents discussion of effects of in-cloud processing based on differences of elemental compositions of individual particles on samples. Specific attention is devoted to processes that add sulfuric acid to particles during in-cloud processing.

2. Field observations and laboratory methods

2.1. Observation site

Observations at Mt. Fuji, Japan were conducted in July and August in 2011 and 2012, during the summer observation campaign period at the Mt. Fuji Weather Station (FWS), which is located at the summit (35.37°N, 138.73°E, 3776 m a.s.l.), and at Tarobo, which is located at the base of Mt. Fuji (35.33°N, 138.81°E, 1284 m a.s.l.). In previous studies, FWS was used to study the gases and aerosols in Mt. Fuji, Japan (Igarashi et al., 2004, 2006; Kaneyasu et al., 2007; Watanabe et al., 2008). In this study, the observations taken on foot were addressed along the mountain path from the summit to Tarobo using a portable optical particle counter and an aerosol sampler. According to cloud conditions of the day, the number concentrations and aerosol samples for analysis of elemental compositions were obtained at altitudes of the top of clouds (close above), in clouds, and immediately under clouds.

2.2. Number concentrations of aerosol particles and cloud droplets

The number–size distribution of atmospheric aerosol particles was measured using a portable laser particle counter (KR-12; RION Co. Ltd.). The laser particle counter (LPC) measures the number concentrations of aerosol particles for six size ranges: diameters greater than 0.3, 0.5, 0.7, 1, 2, and 5 μm . Aerosol particles were counted using the LPC after drying in a diffusion dryer at <30% RH. To quantify tendencies of cloud activation condition in clouds, aerosol number concentrations after removal of cloud droplets using an impactor (PIXI impactor) at the inlet were also measured as cloud interstitial particles. The 50% cut-off diameter (d_{50}) of the droplet-cut impactor stage was 5 μm at a flow rate about 2.73 $\text{l}\cdot\text{min}^{-1}$. The droplet-cut stage was changed manually every 2 min. In this study, the differences between the number concentrations with and without the droplet-cut stage were defined as the number concentrations of cloud droplets. The percentage of cloud droplets (number concentration of cloud droplet particles) to cloud droplets plus aerosol particles (number concentration without the droplet-cut stage) was estimated as the cloud droplet fraction.

2.3. Individual particle analyses using electron microscopy

Aerosol particles were collected for morphological analysis using a transmission electron microscope (TEM). TEM samples

were collected using a sampler that consisted of an inlet, a diffusion drier, two cascade impactors in parallel, and a pump. To analyze the morphological features of aerosol particles, dried (RH < 30%) aerosols were collected using cascade impactors (d_{50} of the two stages were 0.8 μm and 0.2 μm) on carbon-coated nitrocellulose (collodion) films. In this study, samples on the second stage (d_{50} : 0.8 μm diameter) were analyzed. Aerosol samples were collected for 15–20 min at a flow rate about 1.0 $\text{l}\cdot\text{min}^{-1}$ for the cascade impactor. Then TEM samples were taken at about 3–4 altitudes per day based on prevailing weather conditions. To investigate aerosol particles in air mass after disappearance of clouds, samples under cloud/out-of-cloud conditions were collected using the same method as that described above; aerosol particles and cloud droplets were collected as dried particles on the same TEM grid in the impactor downstream of the diffusion drier. The TEM samples were stored under dry conditions at room temperature until TEM analyses were performed at the Tokyo University of Science.

The particles collected on the carbon film were photographed at 1500 \times magnification using a TEM (H-9000NAR; Hitachi Ltd.). To measure the heights of individual particles on the collection surface, particles were coated with a Pt/Pd alloy at a shadowing angle of 26.6 $^\circ$ (arctan 0.5). The Pt/Pd coating thickness was about 7 \AA . Negative films were scanned and recorded with a resolution of 1200 dpi. The scanned image was processed using an image analysis software (Image J) to estimate the projected area of particles (S). Shadow lengths (l) of individual particles were measured manually. The volumes of each particle were calculated from measurements of S and l according to the method described by Okada (1983). The sphere-equivalent diameter of the particles was estimated from the volume.

Elemental compositions of individual particles were analyzed for some particles using an energy-dispersive X-ray (EDX) analyzer used along with a TEM. The analyzer was operated at an accelerating voltage of 200 kV. Elemental analyses were performed for Na, Mg, Al, Si, S, Cl, K, Ca, Ti, Mn, and Fe. The X-ray spectrum was obtained through a detector with a counting time of 120 s. To eliminate the noise effects of the background, a spectrum larger than three times the standard deviation of background spectra measured at a prior test was extracted as the significant spectrum of the particles. The weight percentages of the elemental compositions in individual particles were quantified from the significant spectrum after deduction of the background spectrum near the particles.

2.4. Backward air trajectory and sample selection for in-cloud processing

To identify the impacts of in-cloud processing for the same air mass without scavenging processes, we selected five days as cases (15 July 2011 (case 1), 11 August 2011 (case 2), 26 July 2012 (case 3), 2 August 2012 (case 4), and 9 August 2012 (case 5)) for investigation from nine days of observations, according to meteorological conditions (clouds under upwind conditions without rain) and backward air trajectories (the air mass of sampling sites at the top of clouds and below clouds derived from passage through almost identical courses). Fig. 1 portrays the 72 hour horizontal backward air trajectories for sample sites. Table 1 presents sampling details of altitude, conditions, and measurement results of KR-12 for TEM samples at top-of-

cloud (TOP), in-cloud (IN), and below-cloud (BLW) altitudes. During the observation of case 2, the droplet-cut aerosol sample was also collected under in-cloud conditions as cloud interstitial (CI) samples. The backward trajectory data were computed using the Hybrid Single-Particle Lagrangian Integrated Trajectory (HYSPPLIT 4) model developed by the National Oceanic and Atmospheric Administration (NOAA) Air Resources Laboratory (ARL) (Draxler and Rolph, 2003; Rolph, 2003). Horizontal air trajectories of cases 1 and 4 showed that the air masses were derived from the Pacific Ocean to Mt. Fuji. For cases 2, 3, and 5, the air masses were derived from the western Sea of Japan via western Japan.

2.5. Sampling and analysis of gaseous materials

During 17–22 July 2011, 13–19 July 2012, and 17–23 August 2012, gaseous material (HCl, HNO₂, HNO₃, SO₂, and NH₃) concentrations were measured continuously using alkaline and acid-impregnated cellulose filters at Tarobo. Simultaneous sampling of acidic gases, NH₃, and particulate matter was performed using a four-stage NILU filter holder. The filter pack system comprises a Teflon filter for removing particulate matter, a nylon filter for collecting HNO₃, a sodium-carbonate-impregnated cellulose filter for collecting HNO₂, HCl, and SO₂, and a phosphoric acid-impregnated cellulose filter for collecting NH₃ in series. A potassium carbonate-impregnated cellulose filter was extracted by shaking (500 rpm) with 10 ml of 0.05% H₂O₂ solution and other filters were extracted by shaking (500 rpm) with 10 ml ultrapure water for 30 min. The extracts were filtrated by a 0.45 μm membrane filter and analyzed for NH₄⁺, Cl⁻, NO₃⁻, and SO₄²⁻ by ion chromatography. The sampling times were 6:00–12:00, 12:00–18:00, and 18:00–6:00 for each day. The gaseous material concentrations were analyzed using ion chromatography. More details of the analyses are described by Takeuchi et al. (2003). Unfortunately, the days of observations along the slope of Mt. Fuji on foot were not included in filter sampling periods. To show tendencies of the summer period for the air masses at least, average values of the daytime samples are shown in Table 2. *Maritime* denotes an air mass derived from the Pacific Ocean within a day. *Japan and continental* denotes the other types.

3. Results and discussion

3.1. Number concentrations of aerosol particles and cloud droplets

Fig. 2 shows the number–size distributions of aerosols for the five cases. The size distributions of each day except for case 2 were almost identical for all altitudes. In case 2, the number concentrations of particles less than 1 μm dry diameter were almost identical for all altitudes, but the number concentrations of particles greater than 1 μm dry diameter were higher at higher altitudes. Mt. Fuji is an almost perfect cone. Consequently the mountain path at a higher altitude tends to become crowded. Actually, many climbers visited the summit of Mt. Fuji on that day. Therefore, coarse particles of that day at high altitudes were regarded as containing dust that had been kicked up by climbers. Number concentrations of >0.3 μm of the five cases were 30–150 cm^{-3} . The highest value was that of case 2. The lowest was that of case 4. The cloud droplet fractions

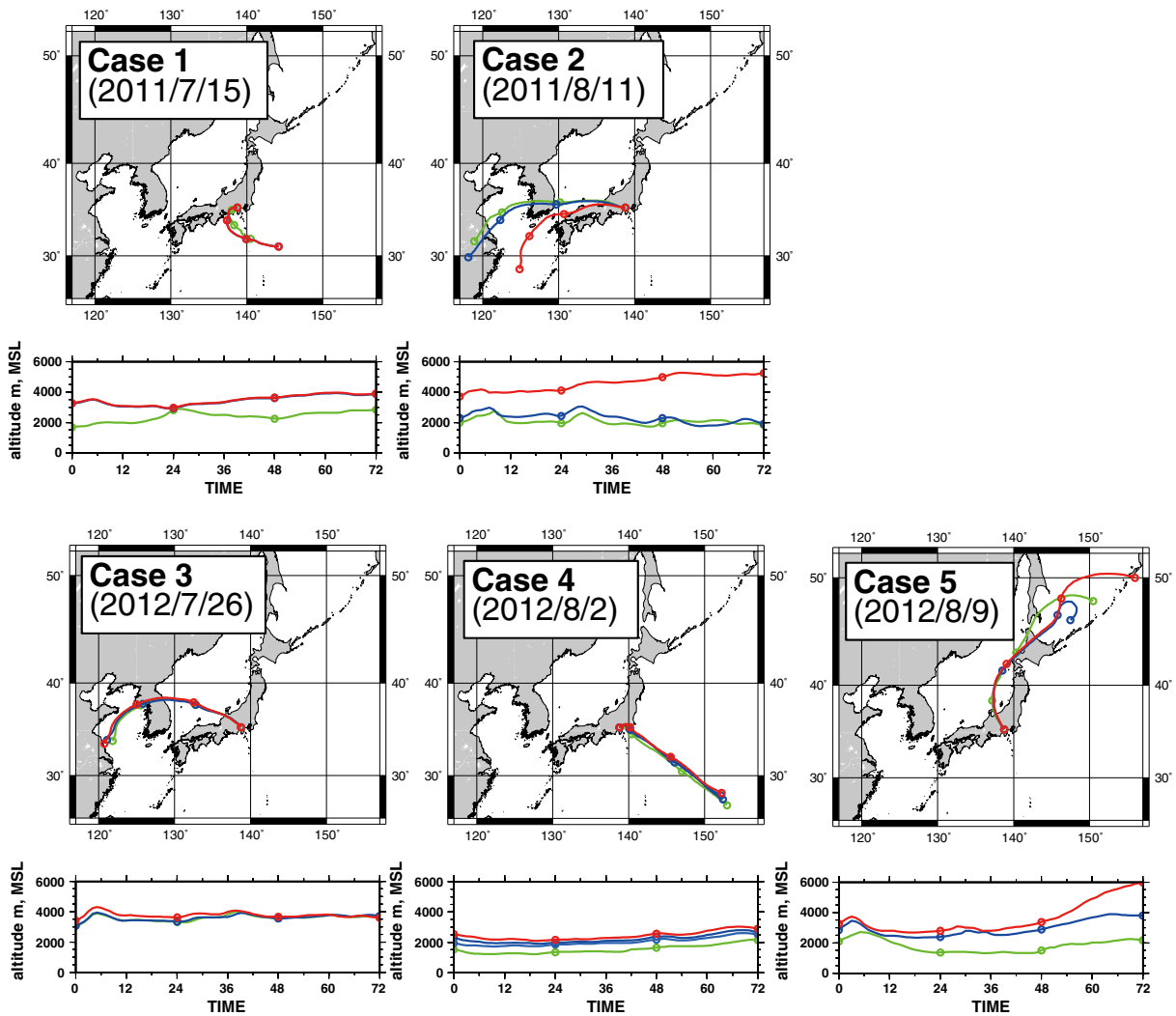


Fig. 1. 72-Hour backward trajectory of air masses for samples. Upper row shows horizontal trajectory starting at the hour of sample collection from the sampling site. Lower row shows vertical profiles of the trajectories.

of $>0.3 \mu\text{m}$ particles under in-cloud conditions were 4–43% (Table 1). The aerosol number concentrations measured using the droplet-cut impactor in the cloud of case 1 were almost identical to those that were measured without using the droplet-cut impactor. This result was obtained because the clouds in case 1 were light; measurements at 2 min intervals were insufficient to clarify the differences of aerosol concentrations between in-cloud and out-of-cloud conditions.

3.2. Individual particle compositions

Fig. 3 presents examples of X-ray spectra of aerosol particles. Particles on the samples were distinguished as those consisting roughly of the following three major aerosol types depicted in Fig. 3: sea salt, dust and sulfate particles. Sea salt particles are composed mainly of NaCl, but Cl^- can be substituted with SO_4^{2-} or NO_3^- . Particles of Fig. 3a have considerably high sodium and chlorine contents compared with the background spectra of the collodion film. Therefore,

they were regarded as sea salt. Particles of Fig. 3b have high sodium, sulfur, and oxygen peak intensities, and do not contain chlorine. In fact, the Na-rich particles without chlorine of Fig. 3b were often found in the samples. They were regarded as sea salt from which chlorine had been displaced completely by sulfate or other materials. Particles rich in silicon, aluminum, and oxygen with minor elements calcium, sulfur, and iron, such as those in Fig. 3c, were found in the samples. The composition suggests that these particles are of crustal origin. Such particles of crustal origin often have an irregular shape, with a long shadow of Pt/Pd. Particles of Fig. 3d were rich in sulfur and oxygen, but they contained no sodium or crustal elements. Such particles were distinguished as sulfate particles. Particles of this type were often prone to be affected by an electron beam, and to be completely or partly evaporated during EDX analysis. Based on the EDX analysis, particles in this study were classified into sea salt, sea-salt with dust, dust, sulfate, and other particles. Sea-salt particle is Na-containing particles without crustal elements (Al, Si and Fe). For particles containing

Table 1

Dates, locations, sampling times for TEM sample, altitude, weather condition and details of LPC data for top-of-cloud (TOP), in-cloud (IN), cloud-interstitial (CI), and below-cloud (BLW) observations at the slope of Mt. Fuji.

Day (Case #)	Sampling time				Cloud information	Particle concentration by LPC					
	Sample type	Start time	Stop time	altitude m a.s.l		Number concentration			Cloud droplet fraction ^a		
						#/cm ³			%		
						>0.3 μm	>0.5 μm	>1 μm	>0.3 μm	>0.5 μm	>1 μm
2011/7/15 (Case 1)	TOP	11:49	11:59	3290	Occasional fog	70.9	3.6	0.6	1	1	9
	IN	12:20	12:30	3255	In light clouds	74.2	3.5	0.5	4	0	2
	BLW	14:21	14:31	1700	Occasional fog	82.7	4.1	0.5	2	2	0
2011/8/11 (Case 2)	TOP	13:55	14:05	3720	Occasional fog	128.1	24.7	7.9	8	34	48
	IN	15:50	16:00	2300	In clouds	123.4	12.2	1.8	8	28	66
	CI	16:30	16:39	2200	In clouds	135.4	12.2	1.5	43	59	83
	BLW	17:11	17:21	2000	Occasional fog	149.6	12.9	0.9	4	9	18
2012/7/26 (Case 3)	TOP	14:50	15:00	3230	Occasional fog	68.9	7.2	0.5	14	11	5
	IN	15:35	15:45	2940	In clouds	112.8	11.8	0.7	18	16	20
	BLW	16:28	16:38	2600	Occasional fog	91.0	10.3	0.5	0	0	–1
2012/8/2 (Case 4)	TOP	15:30	15:48	2550	Occasional fog	42.0	2.2	0.6	10	18	24
	IN a	16:08	16:18	2300	In clouds	39.1	1.8	0.5	16	19	26
	IN b	16:39	16:49	1950	In clouds	33.0	1.7	0.5	4	10	17
	BLW	17:22	17:32	1530	Occasional fog	31.0	2.8	1.0	12	6	5
2012/8/9 (Case 5)	TOP	14:51	15:04	3260	Occasional fog	68.4	5.0	0.4	8	11	14
	IN	15:56	16:06	2870	In clouds	66.7	4.3	0.3	28	35	16
	BLW	16:46	17:06	2100	Occasional fog	103.4	7.0	0.4	16	35	59

^a Cloud droplet fraction is the percentage of cloud droplets to cloud droplets plus aerosol particles, estimated as the number concentration of particles and droplet-cut particles.

the crustal elements, according to a classification method by Nimura et al. (1998), Na-containing particles having a mass ratio of Na/Si in a particle larger than 0.25 are defined as sea-salt particle with dust while others are called dust particles. The sulfate particles are S-containing particles without sodium and crustal elements.

Fig. 4 shows the weight percentages of elemental compositions of individual particles (0.5–2 μm diameter) obtained from TEM samples at the slope of Mt. Fuji. The numbers and percentages of respective particle types are presented in Table 3. For cases 1, 2, 4, and 5, most particles on samples were rich in Na and contained some S and/or Cl, indicating that they mainly comprised sea salt. Most of the Na-rich particles on the BLW sample of case 1 contained Cl, but Cl was not detected for Na-rich particles on the TOP sample. Unlike case 1, most Na-rich particles of cases 2, 4, or 5 were without Cl for all altitudes. Some large (>1 μm) Si-rich particles were also found in the TOP sample of case 2 because of the dust raised by climbers. For the samples of case 3, most particles were small (<1 μm) sulfate particles

Table 2

Concentrations of gaseous materials during summer observation campaigns of 2011 and 2012.

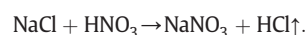
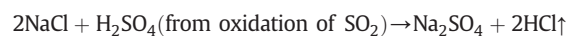
	All periods		Maritime		Japan and continental	
	Number		Number		Number	
	44		31		13	
	Concentration (ppb)					
	avg.	std.	avg.	std.	avg.	std.
HCl	0.24	0.33	0.26	0.37	0.19	0.18
HNO ₂	0.43	0.98	0.43	1.14	0.42	0.28
HNO ₃	0.26	0.16	0.23	0.15	0.33	0.16
SO ₂	0.26	0.26	0.20	0.18	0.37	0.36
NH ₃	2.66	2.42	2.07	2.14	4.08	2.47

and were found without Na. Large (>1 μm) particles were not found in those samples. Some sulfate particles were also found as smaller (<1 μm) particles in samples of cases 2 and 5.

Electron micrographs of TOP, BLW, IN, and CI samples of case 2 are presented in Fig. 5. Major particles of TOP, BLW, and IN samples were dome-like; most were inferred to be sea-salt particles by EDX analysis. However, most cloud interstitial particles (particle on CI sample) were irregularly shaped, comprising mainly Si. Sea-salt particles were not found, indicating that most sea-salt particles of this size range were present as cloud droplets under fog conditions in this case. This result is reasonable because of sea salt's strong propensity to become cloud condensation nuclei.

3.3. Comparison of sea-salt-containing particles in and below clouds

As explained in the previous section, most particles (0.5–2 μm diameter) for the four cases (15 July 2011, 11 August 2011, 2 August 2012, and 9 August 2012) contained sea salt. Because Na in sea salt particles is nonvolatile, the weight/atomic balance of Cl and S to Na has been used as an index for the change of the particle (e.g., Miura et al., 1991; Nimura et al., 1998). NaCl in sea-salt particles can be changed to Na₂SO₄ or NaNO₃ by a displacement reaction with sulfuric acid or nitric acid gas in the atmosphere, as in the following reactions:



This reaction reduces the molar ratio of Cl to Na (Cl/Na) in sea salt particles with increased sulfate and nitrate. Aside

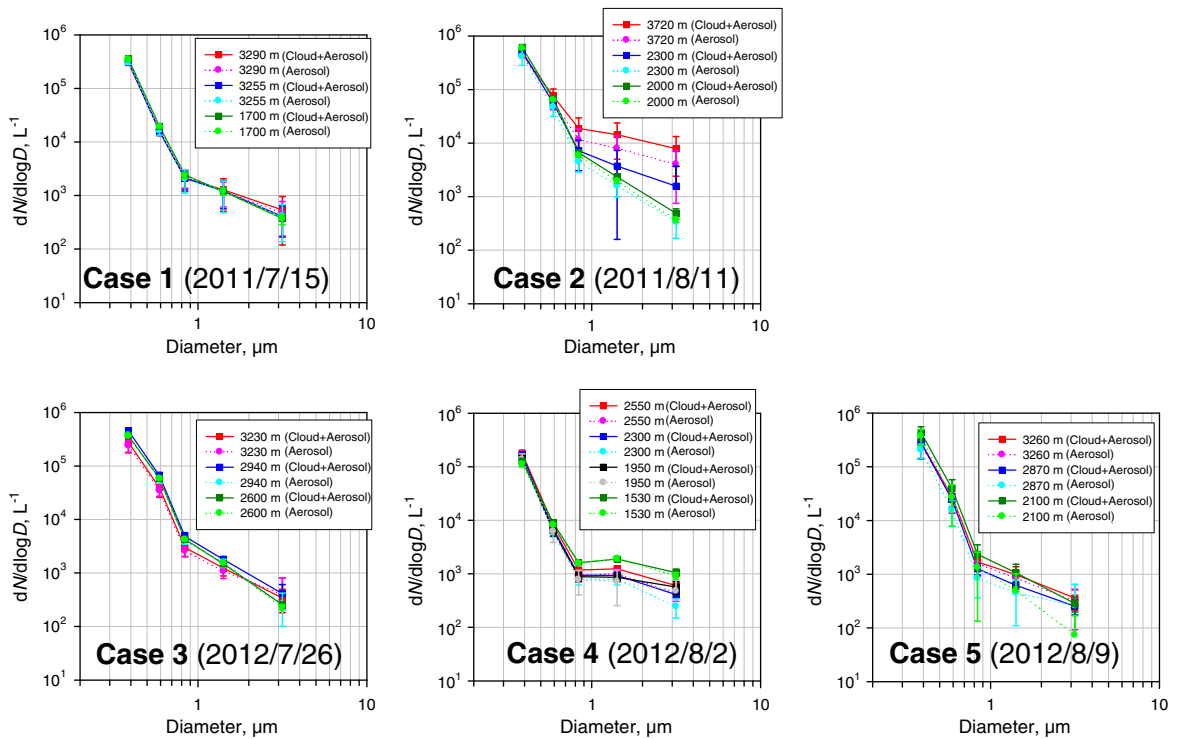


Fig. 2. Number-size distribution of aerosol particles measured at slope of Mt. Fuji. Thin and thick lines respectively represent the total number concentration and number concentration after the cloud-droplet cut.

from the displacement of Cl, the absorption/adsorption to droplet particles and coagulation with another particle can also change the composition of sea salt particles. H_2SO_4 is formed by aqueous-phase SO_2 oxidation in clouds (Liang and Jacobson, 1999; Seinfeld and Pandis, 2006; Warneck, 1999). If such sulfuric acid and non-sea-salt sulfate particles are added to sea-salt particles by absorption and coagulation,

then the molar ratio of S to Na (S/Na) of the particle is altered independent of the change of Cl/Na , unlike the displacement reaction of Cl.

Considering up-wind conditions and small differences of air masses, the differences of relative amounts of S and Cl to Na in sea-salt-containing particles between below-cloud and top-of-cloud altitudes are assumed to be attributable to change

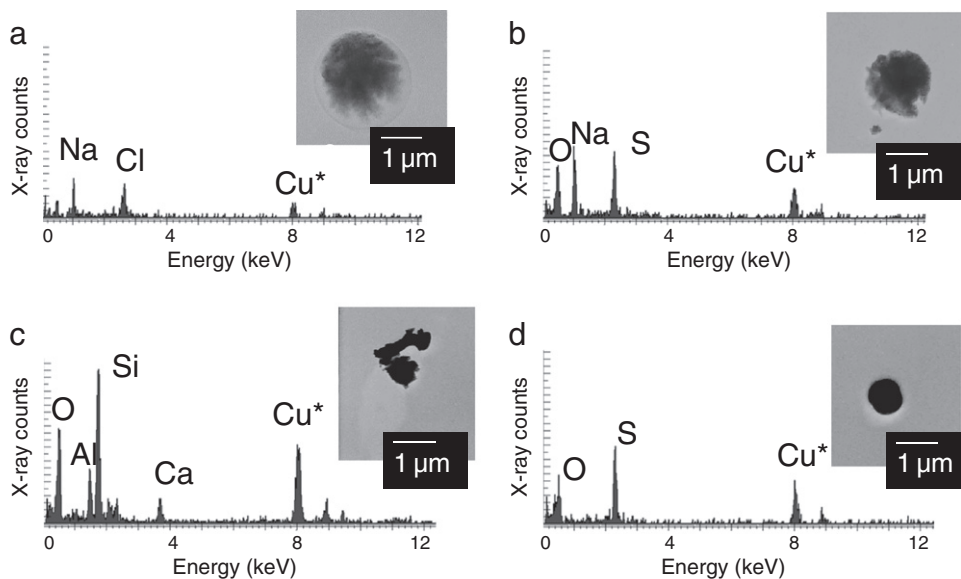


Fig. 3. Typical spectra of energy dispersive X-ray analysis for individual particles collected from the slope of Mt. Fuji: (a) sea-salt particles, (b) sea-salt particles, from which chlorine had been displaced with sulfate, (c) dust particle, and (d) sulfate particle. *Peak of Cu results from the metal film support.

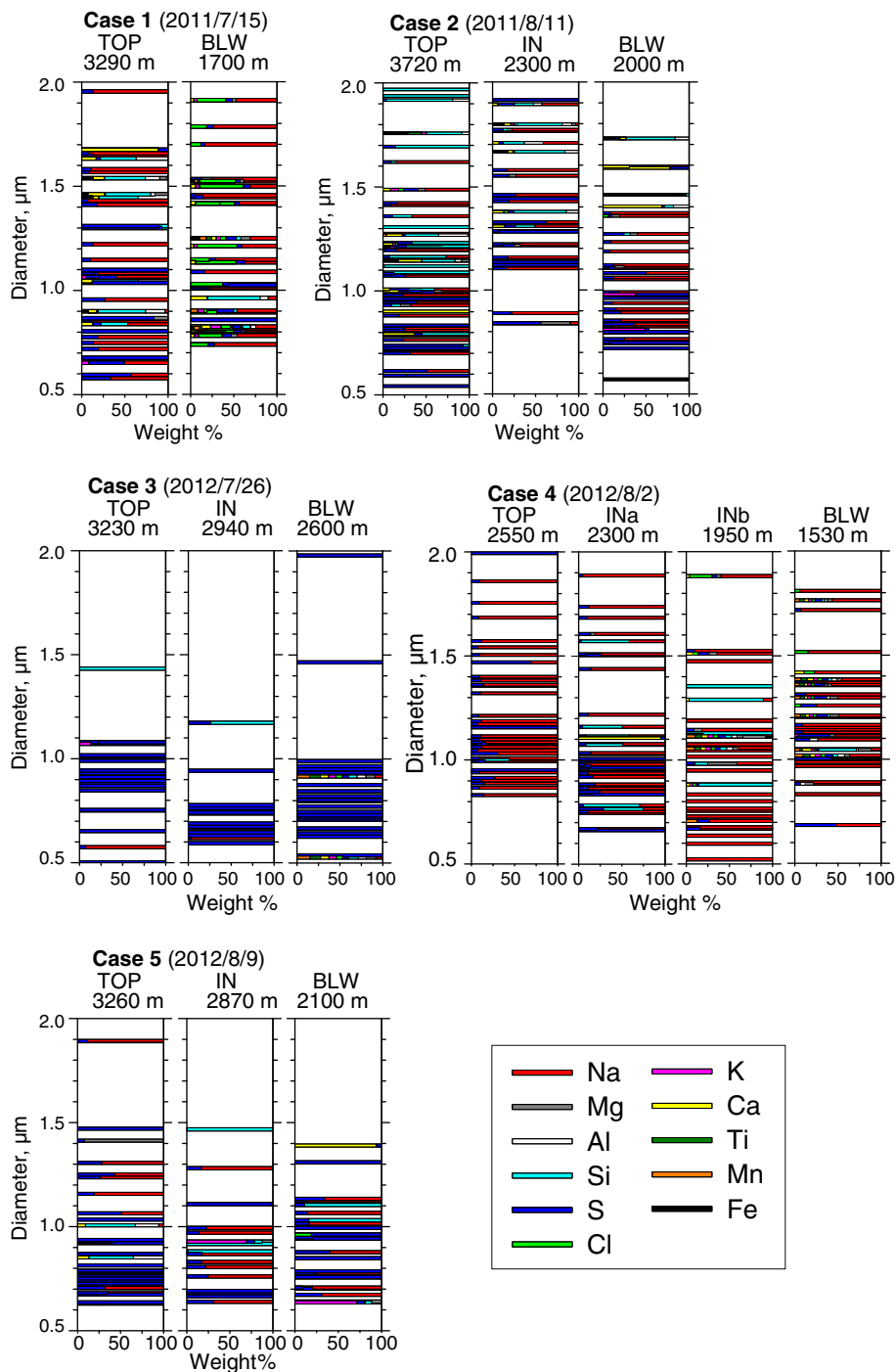


Fig. 4. Relations between particle size and weight percentages of elemental compositions obtained from EDX analysis for samples obtained on the slope of Mt. Fuji.

via in-cloud processing. To assess the change via in-cloud processing of sea-salt particles, we compared the S/Na and Cl/Na ratios in sea-salt-containing particles for different altitudes for cases 1, 2, 4, and 5. The air masses of all altitudes for each case were almost identical based on the trajectories and number size distributions, as explained in the preceding section. Fig. 6 presents the relative weight ratios of Na, Cl, and S for sea-salt-containing particles (sea-salt particles and sea-salt

particles with dust). The analyzed particle number and details of sea-salt-containing particles are presented in Table 4. The solid line in the triangle of Fig. 6 was drawn between compositions that correspond to NaCl and Na₂SO₄. If the sea salt in a particle consists of only NaCl and Na₂SO₄, then the ratio can be expected to be on the solid line. Particles of the plot distributed under the black line can be regarded as particles containing excess of S to that in Na₂SO₄. For all samples in Fig. 6,

Table 3

Number and number fraction of particles classified using EDX analysis.

Case #	Sample type	Analyzed particle number	Particle number and number fraction				
			Sea salt	Sea salt with dust	Dust	Sulfate	Other
Case 1	TOP	39	23 (59%)	1 (3%)	8 (21%)	5 (13%)	2 (5%)
	BLW	33	22 (67%)	8 (24%)	1 (3%)	2 (6%)	0 (0%)
Case 2	TOP	57	28 (49%)	5 (9%)	17 (30%)	6 (11%)	1 (2%)
	IN	29	13 (45%)	6 (21%)	5 (17%)	5 (17%)	0 (0%)
	BLW	35	21 (60%)	2 (6%)	5 (14%)	5 (14%)	2 (6%)
Case 3	TOP	57	6 (11%)	0 (0%)	4 (7%)	36 (63%)	11 (19%)
	IN	29	2 (7%)	0 (0%)	2 (7%)	25 (87%)	0 (0%)
	BLW	35	0 (0%)	3 (8%)	1 (4%)	29 (84%)	1 (4%)
Case 4	TOP	38	34 (89%)	1 (3%)	0 (0%)	3 (8%)	0 (0%)
	INa	43	30 (70%)	8 (19%)	0 (0%)	4 (9%)	1 (2%)
	INb	36	27 (75%)	4 (11%)	4 (11%)	0 (0%)	1 (3%)
	BLW	38	25 (66%)	12 (32%)	0 (0%)	0 (0%)	1 (3%)
Case 5	TOP	48	12 (25%)	1 (2%)	3 (6%)	16 (33%)	16 (33%)
	IN	17	9 (53%)	0 (0%)	4 (24%)	4 (24%)	0 (0%)
	BLW	27	13 (48%)	0 (0%)	3 (11%)	8 (30%)	3 (11%)

most plots were distributed on the upper left side of the line, which implies that Cl in the sea-salt-containing particles was displaced by sulfate and other materials. According to reports describing the ion analyses of bulk samples of aerosols around

the western part of the Japanese Island by Kawakami et al. (2008), the amount of Cl⁻ deficiency in coarse sea salt particles from the seawater ratios was comparable to the sum of equivalent concentrations of NO₃⁻ and non-sea-salt

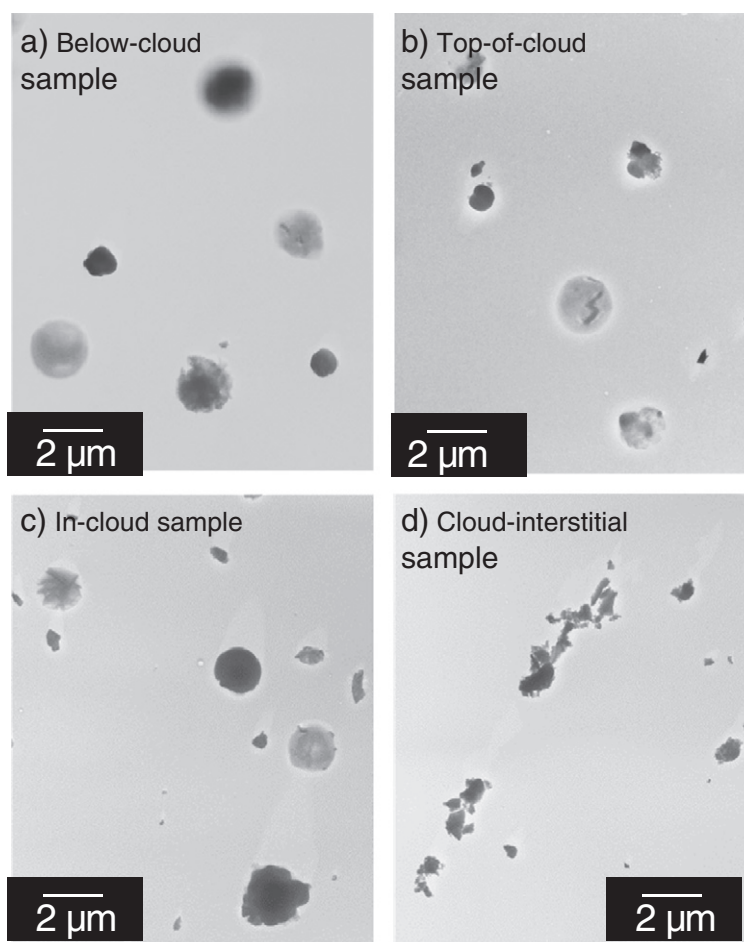


Fig. 5. Electron micrographs of aerosol samples of 11 August 2011 (case 2).

SO_4^{2-} , suggesting Cl^- displacement of sea salt particles by acidic gases such as HNO_3 and SO_2 . Materials that displaced Cl^- in sea-salt-containing particles in this study also seemed reasonable as sulfate and nitrate.

Some sea-salt-containing particles containing Cl were found in the BLW sample at 1700 m a.s.l. for case 1, the INb sample at 1950 m a.s.l., and in the BLW sample at 1530 m a.s.l. for case 4. However, the plots at higher altitudes of cases 1 and 4 were distributed close to a line between Na and S: Cl was not included in sea salts. These samples were collected under up-wind and similar air mass conditions. Therefore, the differences of sea-salt-containing particles for altitudes might be attributed mainly to the displacement reaction in clouds. Fig. 7 portrays median values and 75 and 25 percentiles of Cl/Na and S/Na of sea-salt-containing particles in samples. The median values of Cl/Na and S/Na for 0.5–1 μm and 1–2 μm diameters are presented in Table 3. Although the median values of Cl/Na molar ratios of case 4 were almost zero for all altitudes, those for case 1 differed between altitudes below and at the top of clouds. However, the median values of S/Na for TOP samples of cases 1 and 4 were almost identical to that for BLW samples. Therefore, the differences of Cl/Na ratios with altitude might be attributed mainly to displacement by nitrate under in-cloud conditions.

For the samples of cases 2 and 5, most relative weight ratios of sea-salt-containing particles of all altitudes in Fig. 6

were distributed close to a line between Na and S, suggesting that Cl in sea salt particles on both TOP and BLW samples had already been displaced completely. Naturally, the median values of Cl/Na in Fig. 7 were also almost zero for all altitudes. However, the median values of S/Na for TOP samples were two times higher than that obtained below the clouds. Sea-salt-containing particles in the samples obtained below clouds did not contain Cl. Therefore, the differences of S/Na between below clouds and top of clouds altitudes might be attributed to the addition of sulfate/sulfuric acid onto particles by absorption/adsorption or coagulation under cloud presence conditions.

As presented above, changes of two types in sea-salt-containing particles can be inferred from the results of this study: Cl loss without change in S/Na for cases 1 and 4, and addition of S to sea-salt particles for cases 2 and 5. The air masses of former cases presented in Fig. 1 were derived from the Pacific Ocean. Those of the latter cases were derived from the western Sea of Japan via western Japan. Based on the acidic gaseous materials at Tarobo (1284 m a.s.l.) shown in Table 1, SO_2 and HNO_3 concentrations in maritime air were lower. For the former cases, the presence of Cl-containing sea-salt particles below clouds is explainable if the oxidation gas (i.e. SO_2 and HNO_3 gases) concentrations of maritime air masses were low. Increased S/Na value by in-cloud processing might also differ among the four cases according to the SO_2 concentration. For the latter cases, additional discussion of

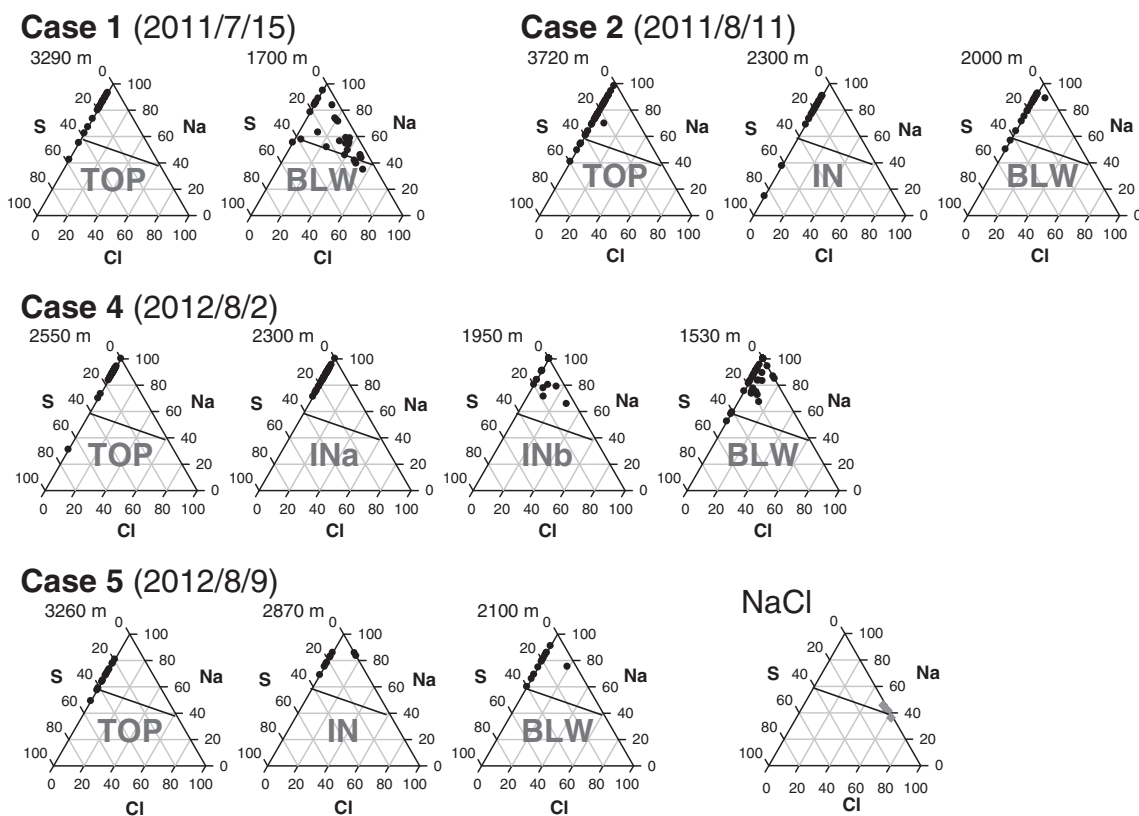


Fig. 6. Relative weight ratios of Na, Cl and S for sea-salt-containing particles in samples of cases 1, 2, 4, and 5. Solid lines in triangles are drawn between compositions corresponding to their ratios of NaCl and Na_2SO_4 .

Table 4

Details of sea-salt containing particles in TEM samples.

Case #	Sample type	Analyzed particle Number		Sea-salt-containing particles									
		0.5–1 μm	1–2 μm	Number		S/Na				Cl/Na			
				0.5–1 μm	1–2 μm	0.5–1 μm		1–2 μm		0.5–1 μm		1–2 μm	
						med	std	med	std	med	std	med	std
Case 1	TOP	17	22	11	13	0.16	0.27	0.11	0.10	0.00	0.00	0.00	0.00
	BLW	16	17	13	17	0.17	0.15	0.09	0.06	0.35	0.24	0.16	0.36
Case 2	TOP	28	29	19	14	0.27	0.24	0.13	0.08	0.00	0.00	0.00	0.02
	IN	3	26	3	16	0.22	2.30	0.15	0.27	0.00	0.00	0.00	0.00
Case 4	BLW	19	16	11	12	0.13	0.10	0.10	0.22	0.00	0.00	0.00	0.01
	TOP	13	25	12	23	0.09	0.09	0.08	0.32	0.00	0.00	0.00	0.00
	INa	28	15	24	14	0.12	0.07	0.08	0.05	0.00	0.00	0.00	0.00
	INb	20	16	18	14	0.00	0.06	0.03	0.06	0.00	0.00	0.00	0.08
Case 5	BLW	14	24	13	24	0.06	0.21	0.07	0.11	0.00	0.04	0.02	0.03
	TOP	38	10	9	7	0.32	0.15	0.26	0.26	0.00	0.00	0.00	0.00
	IN	14	3	8	1	0.18	0.09	–	–	0.00	0.04	–	–
	BLW	21	6	10	3	0.18	0.12	0.12	0.14	0.00	0.05	0.00	0.00

med: median values for sea-salt-containing particles on sample for an altitude.

std: standard deviation for sea-salt-containing particles on sample for an altitude.

the additional effect of sulfuric acid by in-cloud processing is presented in the next section along with estimation of the size change from the particle composition.

3.4. Estimated effects derived from in-cloud processing

As inferred from compositional differences among sea-salt-containing particles on samples of below-cloud and top-of-cloud altitudes, the aerosol particles might be aged by displacement of Cl and the addition of sulfate/sulfuric acid via in-cloud processing. Among these changing processes via in-cloud processing, addition process by absorption and coagulation on the particles can make the particle larger.

For cases 2 and 5, the possibility that particles have been affected by the addition of sulfate/sulfuric acid without displacement of Cl was shown by comparing samples for altitudes. The addition of sulfate/sulfuric acid to sea-salt particles can alter the particle size with changes of the particle composition; the S/Na ratio of sea-salt-containing particles is useful as an indicator of the additional sulfate/sulfuric acid.

Using median values of S/Na measured from samples of cases 2 and 5, one can estimate the additional mass fraction of sulfuric acid to a particle by in-cloud processing from BLW to TOP altitudes. For our estimation, we assumed that (1) the particles before in-cloud processing consisted of Na_2SO_4 and NaNO_3 , (2) the particles after in-cloud processing consisted

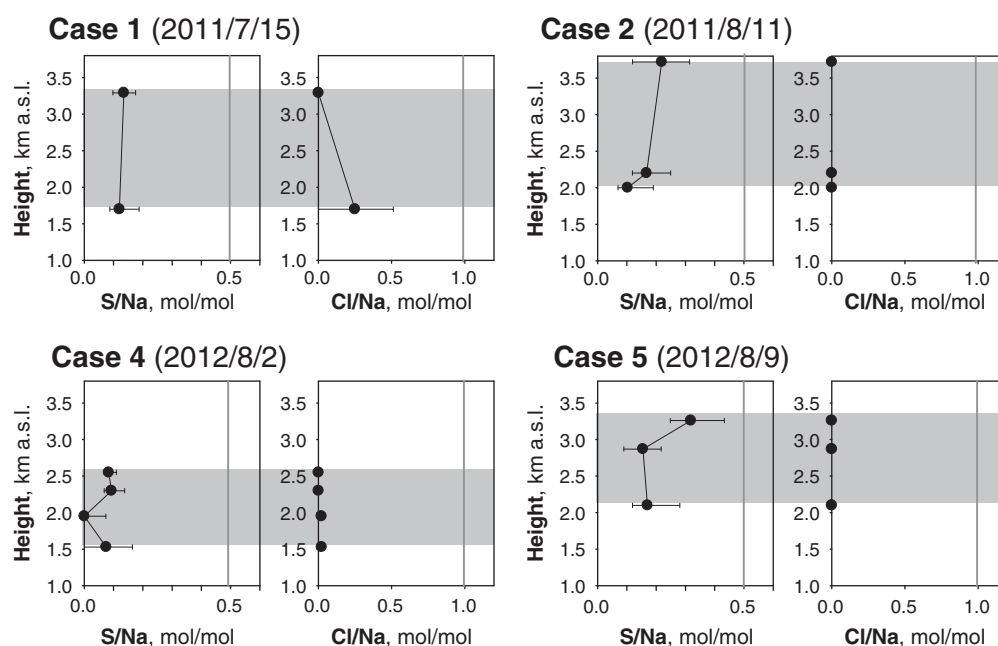


Fig. 7. Relations between altitudes and molar ratio of Cl/Na and S/Na of sea-salt-containing particles. Closed dots show median values for respective samples. Left and right error bars respectively show the 25th percentile and the 75th percentile. Gray areas denote altitudes of fog conditions (cloud presence).

of H_2SO_4 , Na_2SO_4 and NaNO_3 and (3) the amounts of NO_3^- and Na^+ in a particle were constant before and after in-cloud processing. Based on those assumptions, the mass and size ratios (R_m and R_d , respectively) of particles above clouds to that below clouds can be written as shown below.

$$R_m = \frac{m_{\text{TOP}}}{m_{\text{BLW}}} = \frac{\frac{1}{2}r_{\text{BC}}M_{\text{Na}_2\text{SO}_4} + (1-r_{\text{BLW}})M_{\text{NaNO}_3} + (r_{\text{TOP}}-r_{\text{BLW}})M_{\text{H}_2\text{SO}_4}}{\frac{1}{2}r_{\text{BLW}}M_{\text{Na}_2\text{SO}_4} + (1-r_{\text{BLW}})M_{\text{NaNO}_3}} \quad (1)$$

$$R_d = \frac{d_{\text{TOP}}}{d_{\text{BLW}}} = \left(\frac{\frac{1}{2}r_{\text{BLW}} \frac{M_{\text{Na}_2\text{SO}_4}}{\rho_{\text{Na}_2\text{SO}_4}} + (1-r_{\text{BLW}}) \frac{M_{\text{NaNO}_3}}{\rho_{\text{NaNO}_3}} + (r_{\text{TOP}}-r_{\text{BLW}}) \frac{M_{\text{H}_2\text{SO}_4}}{\rho_{\text{H}_2\text{SO}_4}}}{\frac{1}{2}r_{\text{BLW}} \frac{M_{\text{Na}_2\text{SO}_4}}{\rho_{\text{Na}_2\text{SO}_4}} + (1-r_{\text{BLW}}) \frac{M_{\text{NaNO}_3}}{\rho_{\text{Na}_2\text{SO}_4}}} \right)^{\frac{1}{3}} \quad (2)$$

Therein, m_{TOP} and m_{BLW} respectively represent the particle masses at TOP and BLW altitudes. Furthermore, d_{TOP} and d_{BLW} respectively stand for particle sizes at TOP and BLW altitudes. M_X and ρ_X respectively denote the molecular mass and density of material X. Also, r_{TOP} and r_{BLW} respectively signify the median values of S/Na for TOP and BLW samples measured in this study using EDX analysis. Based on calculations using the equations presented above, the R_m and R_d values of case 1 were 1.14 and 1.06 for 0.5–1 μm particles and 1.03 and 1.01 for 1–2 μm particles, respectively. Those of case 5 were 1.12 and 1.05 for 0.5–1 μm particles and 1.15 and 1.06 for 1–2 μm particles, respectively. By converting the results into the volume change per unit distance, the changes were found to be 0.03 and 0.02 $\mu\text{m}^3/\text{km}$, respectively, for 0.5–1 μm and 1–2 μm of case 1, and 0.04 and 0.18 $\mu\text{m}^3/\text{km}$, respectively, for 0.5–1 μm and 1–2 μm of case 5. As shown in Table 1, the number fractions of cloud droplets to aerosol and cloud particles (cloud droplets fraction) under in-cloud conditions were less than 50% for diameter greater than 0.3 μm . The cloud droplet fraction suggests that possible supersaturation in the cloud was less than or comparable to that of stratus and stratocumulus clouds. Assuming a typical updraft velocity of 0.05 m/s for stratus and stratocumulus clouds (Venkataraman et al., 2001), the rate of volume change of a particle in this study was estimated as 1.4×10^5 – $6.4 \times 10^5 \mu\text{m}^3/\text{h}$.

Although the two cases were days with larger changes of S/Na ratios in this study, the estimation revealed that size changes during in-cloud processing in this study were smaller than 6% in this size range. Actually, the clearer shift of number size distribution from BLW to TOP altitude was not observed on 9 August 2012 in Fig. 2. Estimated values for size changes agree reasonably well with the observed number concentration. The modification of aerosol sizes by cloud processing was also discussed empirically by comparing cloud upwind and downwind particle size distributions (Bower et al., 1997, 2000; Choularton et al., 1997; Mertes et al., 2005), but the changes of aerosol sizes were detected only for particles with diameters of less than 300 nm. In this study, the change by in-cloud processing, which was distinguished only slightly by number–size distributions, was estimated by tracing S/Na ratios of aerosol particles obtained at different altitudes with respect to clouds. The estimation reported in this study demonstrates the usefulness of the analysis of individual particles to support

quantitative evaluation of changes in a particle by aging processes.

4. Summary and conclusions

Atmospheric aerosol particles below clouds, in clouds, and at tops of clouds were observed along the slope of Mt. Fuji in Japan using a portable laser particle counter (LPC) and an aerosol sampler. To elucidate differences of aerosol particles before and after in-cloud processing, individual particles (0.5–2 μm diameter) of samples from the five cases (days) collected at different altitudes under similar backward air mass trajectory conditions were analyzed using a TEM equipped with an EDX analyzer.

Most particles in the samples of the four cases were sea-salt-containing particles. Those particles in the samples of the other case were sulfate particles. Compositions of sea-salt-containing particles for the former four cases differed according to altitudes with respect to clouds. In two cases for air mass from the Pacific Ocean, Cl was detected from some sea-salt-containing particles on the below-cloud samples, although sea-salt-containing particles of top-of-cloud samples did not contain Cl. This result suggests that Cl in the sea-salt-containing particles was displaced by other elements in the clouds. In the other two cases for air mass from inland of Japan, sea-salt-containing particles in samples of all altitudes did not contain Cl. However, molar ratios of S to Na of sea-salt-containing particles at top-of-cloud altitudes tended to be higher than those below clouds, suggesting that some sulfate/sulfuric acid was added to the sea-salt-containing particles after complete displacement of Cl by absorption of SO_2 or coagulation with sulfate. The effects on particle size and volume of the addition of sulfuric acid by in-cloud processing were estimated using the molar ratios of S to Na of sea-salt-containing particles obtained at below-cloud and top-of-cloud altitudes. The estimation revealed that size changes during in-cloud processing from below-cloud to top-of-cloud altitudes were less than 6% in this size range for diameters of 0.5–2 μm . Effects of in-cloud processes found in this study are expected to be useful for evaluating the aerosol transition and material cycle via clouds.

Acknowledgments

We are indebted to S. Matsuyama and T. Isobe of the Faculty of Science and Engineering, Waseda University for the chemical analyses of gaseous materials. We gratefully acknowledge the NOAA Air Research Laboratory (ARL) for the provision of the HYSPLIT transport and dispersion model. This study was conducted during the period when the non-profit organization 'Valid Utilization of Mt. Fuji Weather Station' had received a part of the Mt. Fuji Weather Station from the Japan Meteorological Agency and managed it. This study was partly supported by the Grants-in-Aid for Scientific Research, Category C (Grant No. 22510019), from JSPS.

References

- Birmili, W., Yuskiewicz, B., Wiedensohler, A., Stratmann, F., Choularton, T.W., Bower, K.N., 1999. Climate-relevant modification of the aerosol size distribution by processes associated with orographic clouds. *Atmos. Res.* 50, 241–263.

- Bower, K.N., Choulaton, T.W., Gallagher, M.W., Colvile, R.N., Wells, M., Beswick, K.M., Wiedensohler, A., Hansson, H.-C., Svenningsson, B., Swietlicki, E., Wendisch, M., Berner, A., Krusiz, C., Laj, P., Facchini, M.C., Fuzzi, S., Bizjak, M., Dollard, G., Jones, B., Acker, K., Wipreht, W., Preiss, M., Sutton, M.A., Hargreaves, K.J., Storeton-West, R.L., Cape, J.N., Arends, B.G., 1997. Observations and modelling of the processing of aerosol by a hill cap cloud. *Atmos. Environ.* 31 (16), 2527–2543.
- Bower, K.N., Choulaton, T.W., Gallagher, M.W., Beswick, K.M., Flynn, M.J., Allen, A.G., Davison, B.M., James, J.D., Robertson, L., Harrison, R.M., Frank, G., Swietlicki, E., Zhou, J., Berg, O.H., Menten, B., Papaspiouos, Hansson, H.-C., Leck, C., Kulmala, M., Aalto, P., Väkevä, M., Berner, A., Bizjak, M., Fuzzi, S., Laj, P., Facchini, M.-C., Orsi, G., Ricci, L., Nielsen, M., Allan, B.J., Coe, H., McFiggans, G., Plane, J.M.C., Collett Jr., J.L., Moore, K.F., Sherman, D.E., 2000. ACE-2 HILLCLOUD. An overview of the ACE-2 ground-based cloud experiment. *Tellus* 52B, 750–778.
- Choulaton, T.W., Colvile, R.N., Bower, K.N., Gallagher, M.W., Wells, M., Beswick, M.W., Arends, B.G., Möls, J.J., Kos, P.A., Fuzzi, S., Lind, J.A., Orsi, G., Facchini, M.C., Laj, P., Gieray, R., Wieser, P., Engelhardt, T., Berner, A., Krusiz, C., Moller, D., Acker, A., Wipreht, W., Lutke, J., Levsen, K., Bizjak, M., Hansson, H.-C., Cederfelt, S.-I., Frank, G., Menten, D., Martinsson, B., Orsini, D., Svenningsson, B., Swietlicki, E., Wiedensohler, A., Noone, K.J., Pahl, S., Winkler, P., Seyffer, E., Helas, G., Jaeschke, W., Georgii, H.W., Wobrock, W., Preiss, M., Maser, R., Schell, D., Dollard, G., Jones, B., Davies, T., Sedlak, D.L., David, M.M., Wendisch, M., CaDe, J.N., Hamreaves, K.J., Sutton, M.A., Storeton-West, R.L., Fowler, D., Hallberg, A., Harrison, R.M., Peak, J.D., 1997. The Great Dun Fell Cloud experiment 1993: an overview. *Atmos. Environ.* 31, 2393–2405.
- Draxler, R.R., Rolph, G.D., 2003. HYSPLIT Hybrid Single-Particle Lagrangian Integrated Trajectory Model access via NOAA ARL READY Website <http://www.arl.noaa.gov/ready/hysplit4.html>. NOAA Air Resources Laboratory, Silver Spring, MD.
- Fuchs, N.A., 1964. The coagulation of aerosols. *The Mechanics of Aerosols*. Dover Publications, Inc., New York, pp. 288–322.
- Haywood, J.M., Boucher, O., 2000. Estimate of the direct and indirect radiative forcing due to tropospheric aerosols: a review. *Rev. Geophys.* 38, 513–543.
- Huang, X.F., Yu, J.Z., 2008. Size distribution characteristics of elemental carbon in the atmosphere of coastal urban area in South China: characteristics, evolution processes, and implications for the mixing state. *Atmos. Chem. Phys.* 8, 5843–5853.
- Husar, R.B., Whitby, K.T., 1973. Growth mechanisms and size spectra of photochemical aerosols. *Environ. Sci. Technol.* 7, 241–247.
- Igarashi, Y., Sawa, Y., Yoshioka, K., Takahashi, H., Matsueda, H., Fujii, K., Dokiya, Y., 2004. Monitoring the SO₂ concentration at the summit of Mt. Fuji and a comparison with other trace gases during winter. *J. Geophys. Res.* 109, D17304.
- Igarashi, Y., Sawa, Y., Yoshioka, K., Takahashi, H., Matsueda, H., Dokiya, Y., 2006. Seasonal variations in SO₂ plume transport over Japan: observations at the summit of Mt. Fuji from winter to summer. *Atmos. Environ.* 40, 7018–7033.
- Kaneyasu, N., Igarashi, Y., Sawa, Y., Takahashi, H., Takada, H., Kumata, H., Höller, R., 2007. Chemical and optical properties of 2003 Siberian forest fire smoke observed at the summit of Mt. Fuji, Japan. *J. Geophys. Res.* 112, D13214.
- Kawakami, N., Osada, K., Nishita, C., Yabuki, M., Kobayashi, H., Hara, K., Shiobara, M., 2008. Factors controlling sea salt modification and dry deposition of nonsea-salt components to the ocean. *J. Geophys. Res.* 113. <http://dx.doi.org/10.1029/2007JD009410>.
- Kerminen, V.-M., Wexler, A.S., 1995. Growth laws for atmospheric aerosol particles: an examination of the bimodality of the accumulation mode. *Atmos. Environ.* 29, 3263–3275.
- Kojima, T., Buseck, P.R., 2005. Aerosol particles from tropical convective systems: 2. Cloud bases. *J. Geophys. Res.* 110. <http://dx.doi.org/10.1029/2004JD005173>.
- Kojima, T., Buseck, P.R., Wilson, J.C., Reeves, J.M., Mahoney, M.J., 2004. Aerosol particles from tropical convective systems: cloud tops and cirrus anvils. *J. Geophys. Res.* 109. <http://dx.doi.org/10.1029/2003JD004504>.
- Li, W., Li, P., Sun, G., Zhou, S., Yuan, Q., Wang, W., 2011. Cloud residues and interstitial aerosols from non-precipitating clouds over an industrial and urban area in northern China. *Atmos. Environ.* 45, 2488–2495.
- Liang, J., Jacobson, M.Z., 1999. A study of sulfur dioxide oxidation pathways over a range of liquid water contents, pH values, and temperatures. *J. Geophys. Res.* 104, 13 749–13 769.
- Mamane, Y., Gottlieb, J., 1989. The study of heterogeneous reactions of carbonaceous particles with sulfur and nitrogen oxides using single particles. *J. Aerosol Sci.* 20, 575–584.
- Matsuki, A., Schwarzenboeck, A., Venzac, H., Laj, P., Crumeyrolle, S., Gomes, L., 2010. Cloud processing of mineral dust: direct comparison of cloud residual and clear sky particles during AMMA aircraft campaign in summer 2006. *Atmos. Chem. Phys.* 10, 1057–1069.
- Meng, Z., Seinfeld, J.H., 1994. On the source of submicrometer droplet mode of urban and regional aerosols. *Aerosol Sci. Technol.* 20, 253–265.
- Mertes, S., Galgon, D., Schwirn, K., Nowak, A., Lehmann, K., Massling, A., Wiedensohler, A., Wipreht, W., 2005. Evolution of particle concentration and size distribution observed upwind, inside and downwind hill cap clouds at connected flow conditions during FEBUKO. *Atmos. Environ.* 39, 4233–4245.
- Miura, K., Kumakura, T., Sekikawa, T., 1991. The effect of continental air mass on the modification of individual sea-salt particles collected over the coast and the open sea. *J. Meteorol. Soc. Jpn.* 69, 429–438.
- Nimura, N., Okada, K., Fan, X.-B., Kai, K., Arai, K., Shi, G.-Y., Takahashi, S., 1998. Formation of Asian dust-storm particles mixed internally with sea salt in the atmosphere. *J. Meteorol. Soc. Jpn.* 76, 275–288.
- Okada, K., 1983. Nature of individual hygroscopic particles in the urban atmosphere. *J. Meteorol. Soc. Jpn.* 61, 727–735.
- Piliinis, C., Pandis, S.N., Seinfeld, J.H., 1995. Sensitivity of direct climate forcing by atmospheric aerosols to aerosol size and composition. *J. Geophys. Res.* 100D9, 18739–18754.
- Pósfai, M., Simonic, R., Li, J., Hobbs, P.V., Buseck, P.R., 2003. Individual aerosol particles from biomass burning in southern Africa: 1. Compositions and size distributions of carbonaceous particles. *J. Geophys. Res.* 108, D13. <http://dx.doi.org/10.1029/2002JD002291>.
- Rolph, G.D., 2003. Real-time environment applications and display system READY. NOAA Air Resour. Lab., Silver Spring, MD (Available at <http://www.arl.noaa.gov/ready/hysplit4.html>).
- Seinfeld, J.H., Pandis, S.N., 2006. *Atmospheric Chemistry and Physics, From Air Pollution to Climate Change*, Second ed. John Wiley and Sons, Inc., New York (1203 pp.).
- Takeuchi, M., Okochi, H., Igawa, M., 2003. Deposition of coarse soil particles and ambient gaseous components dominating dew water chemistry. *J. Geophys. Res.* 108 (D10), 4319–4323.
- Twohy, C.H., Anderson, J.R., 2008. Droplet nuclei in non-precipitating clouds: composition and size matter. *Environ. Res. Lett.* 3, 1–9.
- Twomey, S., 1977. *Atmospheric Aerosols, Developments in Atmospheric Science*, 7. Elsevier, New York (302 pp.).
- Ueda, S., Osada, K., Takami, A., 2011a. Morphological features of soot-containing particles internally mixed with water-soluble materials in continental outflow observed at Cape Hedo, Okinawa, Japan. *J. Geophys. Res.* 116.
- Ueda, S., Osada, K., Okada, K., 2011b. Mixing states of cloud interstitial particles between water-soluble and insoluble materials at Mt. Tateyama, Japan: effect of meteorological conditions. *Atmos. Res.* 99, 325–336.
- Venkataraman, C., Mehra, A., Mhaskar, P., 2001. Mechanisms of sulphate aerosol production in clouds: effect of cloud characteristics and season in the Indian region. *Tellus* 53B, 260–272.
- Warneck, P., 1999. The relative importance of various pathways for the oxidation of sulphur dioxide and nitrogen dioxide in sunlit continental fair weather clouds. *Phys. Chem. Chem. Phys.* 1, 5471–5483.
- Watanabe, K., Takebe, Y., Sode, N., Igarashi, Y., Takahashi, H., Dokiya, Y., 2008. Fog and rain water chemistry at Mt. Fuji: a case study during the September 2002 campaign. *Atmos. Res.* 82, 652–662.
- Xiao, R., Takegawa, N., Kondo, Y., Miyazaki, Y., Miyakawa, T., Hu, M., Shao, M., Zeng, L.M., Hofzumahaus, A., Holland, F., Lu, K., Sugimoto, N., Zhao, Y., Zhang, L.M., 2009. Formation of submicron sulfate and organic aerosols in the outflow from the urban region of the Pearl River Delta in China. *Atmos. Environ.* 43, 3754–3764.